Class. Quantum Grav. **13** (1996) 433–460. Printed in the UK

Topology and classical geometry in (2+1) gravity

R Franzosi and E Guadagnini

Dipartimento di Fisica dell'Università di Pisa, Istituto Nazionale di Fisica Nucleare, Sezione di Pisa, 2 Piazza Torricelli, 56100 Pisa, Italy

Received 7 August 1995, in final form 14 December 1995

Abstract. The structure of the spacetime geometry in $(2+1)$ gravity is described by means of a foliation in which the space-like surfaces admit a tessellation made of polygons. The dynamics of the system is determined by a set of 't Hooft's rules which specify the time evolution of the tessellation. We illustrate how the non-trivial topology of the universe can be described by means of 't Hooft's formalism. The classical geometry of a universe with the spatial topology of a torus is considered and the relation between 't Hooft's transitions and modular transformations is discussed. The universal covering of spacetime is constructed. The non-trivial topology of an expanding universe gives origin to a redshift effect; we compute the value of the corresponding 'Hubble's constant'. Simple examples of tessellations for universes with the spatial topology of a surface with higher genus are presented.

PACS numbers: 0420G, 0450

1. Introduction

In $(2 + 1)$ dimensions, the Riemann tensor can be expressed in terms of the Ricci tensor; consequently, vanishing of the Einstein tensor implies [1] vanishing of spacetime curvature. Thus, in the absence of matter, spacetime can be represented by the union of simply connected domains with appropriate identifications of their boundaries; each domain is isometrically equivalent to a region of the three-dimensional Minkowski space $\mathcal{M}$. In this representation of spacetime, the dynamics of the system together with the information on the topology of the universe and the causal structure of spacetime are encoded in the gluing homeomorphisms which describe how the boundaries of the different domains must be identified and how the associated tangent spaces are related. The problem of constructing a consistent set of gluing homeomorphisms has recently been considered and solved by 't Hooft [2]. In this article we shall use 't Hooft's formalism to describe, in $(2+1)$ gravity, the classical geometry of universes with the topology of $\Sigma_g \times \mathbb{R}$, where Σ_g denotes a Riemann surface of genus $g \geqslant 1$.

The physical systems that we shall study have already been considered in the literature. In particular, the Arnowitt, Deser and Misner (ADM) reduction [3] of the Einstein equations in $(2 + 1)$ dimensions to a Hamiltonian system over Teichmüller space has been discussed by Martinec [4], by Moncrief [5] and by Hosoya and Nakao [6]. Thus, the original parts of our work are essentially related to the use of 't Hooft's formalism [2]. This formalism is particularly convenient for doing computations and computer simulations [2] in $(2+1)$ gravity. The 't Hooft solution of classical $(2+1)$ gravity (possibly in the presence of gravitating spinless particles) is based on the peculiar symmetry properties of general relativity in $(2 + 1)$ dimensions and suggests interesting developments [7] at the quantum level.

0264-9381/96/030433+28$19.50 © 1996 IOP Publishing Ltd

After a brief introduction to the main aspects of 't Hooft's formulation, we shall give a detailed description of the classical geometry of a universe with the spatial topology of a torus. We shall discuss the relation between 't Hooft's transitions, which appear in the evolution of the tessellation, and modular transformations. The covering space of spacetime will be constructed and the appearance of a redshift effect, which is induced by the non-trivial topology of an expanding universe, will be considered. We shall use the structure of the covering space to compute the value of the corresponding 'Hubble's constant'. Finally, we will give simple examples of tessellations for universes with the topology of a surface with higher genus.

Several methods have been proposed to study gravity in $(2+1)$ dimensions; we shall not elaborate here on the relations between these various formalisms. We only note that the 't Hooft version of $(2+1)$ gravity is strictly connected with (and could be understood as a partially gauge-fixed version of) the covariant formulation [8] of Waelbroeck. This covariant formulation plays an important role in $(2+1)$ gravity because it is also related to the Chern–Simons interpretation [9,10] of $(2+1)$ gravity, to Ashtekar's approach based on connections [11, 12] and to the algebraic construction [13] of Nelson and Regge.

2. Evolution of the tessellation

In this section we shall recall the main features of the 't Hooft presentation of spacetime which will be used in the next sections. One considers a spacetime foliation in which each space-like surface $\Sigma(t)$ is described by means of a tessellation [2] made of polygons, as shown in figure 1. We shall firstly concentrate on a pure gravity system; the introduction of matter will be discussed later. A Lorentz frame is associated with each polygon; with respect to this frame, the interior of each polygon coincides with an open domain of the surface defined by the relation $t = \text{constant}$. The hedges of adjacent polygons must be identified. Each edge may be static or may have a constant velocity in the direction which is orthogonal to the edge itself. Two edges which must be identified have necessarily the same length and the same velocity; moreover, for both edges this velocity is directed inside or outside the polygon. Because of the constant velocities of the edges, the length of each edge is a linear function of time and the angles between edges are constant in time.

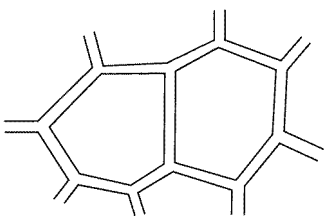

Figure 1. Detail of a tessellation made of polygons.

In order to specify the structure of the tangent space and how the different Lorentz frames are related, we only need to consider how tensors are modified under a parallel transport along an oriented path which crosses two edges which must be identified. Let us introduce an holonomy matrix $H \in SO(2,1)$ which describes the effects of the parallel transport of vectors [14]. If one denotes by η the rapidity parameter corresponding to the

velocity of two edges which must be identified, the holonomy associated with a crossing of these edges is a boost [2] with rapidity parameter (2η) along the orthogonal direction. As shown by 't Hooft [2], this rule can be interpreted as a kinematic condition which is related to the causal structure of spacetime.

When the length of one of the edges vanishes or when one of the corners hits an edge, one has a transition in which the structure of the tessellation of $\Sigma(t)$ undergoes a local change. As discussed by 't Hooft in [2], the transitions which describe the local modifications of the tessellation are shown in figure 2. In a transition of type A, two edges which must be identified shrink to zero and a new couple of edges is formed; this process corresponds to an exchange of vertices. In a transition of type D one has a split due to a vertex which hits two edges. A transition of type F describes a vertex grazing; this transition differs from a type A transition because one of the vertex angles is greater than π. Finally, in the transitions of types G and J one has a triangle or a double triangle disappearance. Thus, the time evolution of the space-like surface $\Sigma(t)$ is described by a sequence of 't Hooft transitions and, within two consecutive transitions, the evolution of the size of polygons is linear in time. The rules which must be used to determine the local changes of the tessellation in the transitions have been described by 't Hooft in [2]. These rules, which specify the velocities and the angles of the edges which are formed in the transitions, are consequences of the vertex conditions. The vertex conditions ensure that the spacetime described by the time evolution of the tessellation corresponds to a solution of the Einstein equations.

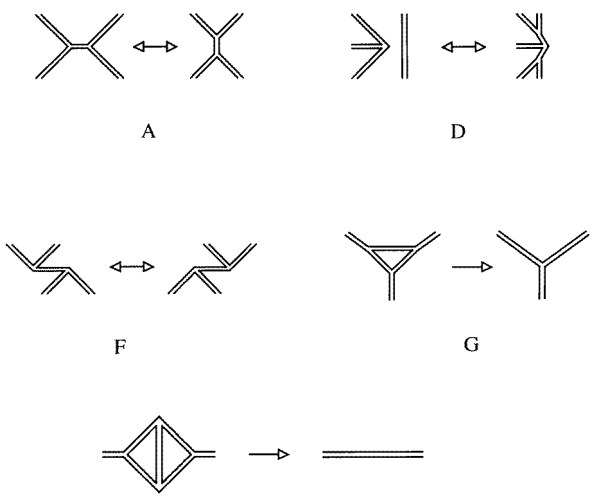

Figure 2. The five types of 't Hooft transition.

The points in which three or more couples of edges meet are called vertices. One can always choose the tessellation of the Cauchy surfaces in such a way that only 3-valent vertices occur. Since the Riemann tensor must vanish in each vertex, the holonomy associated with a loop enclosing a vertex must be represented by the identity matrix. This constraint introduces a set of relations called vertex conditions. Consider the vertex shown in figure 3; the rapidity parameters corresponding to the velocities of the edges are denoted by $\{\eta_i\}$ with $i = 1, 2, 3$ and $\{\alpha_i\}$ are the angles between the edges.

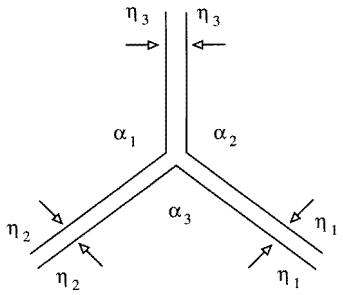

Figure 3. Three-valent vertex and the corresponding parameters.

In terms of the variables

$$\mathrm{Ch}\,2\eta_i = \gamma_i, \qquad \mathrm{Sh}\,2\eta_i = \sigma_i, \tag{2.1}$$

$$\cos\alpha_i = c_i, \qquad \sin\alpha_i = s_i \tag{2.2}$$

the vertex conditions take the form [2, 14]

$$\gamma_1\gamma_3 + c_2\sigma_1\sigma_3 = \gamma_2, \tag{2.3}$$

$$-\sigma_3\gamma_1 - c_2\sigma_1\gamma_3 = c_1\sigma_2, \tag{2.4}$$

$$s_2\sigma_1 = s_1\sigma_2, \tag{2.5}$$

$$-\sigma_1\gamma_3 - c_2\sigma_3\gamma_1 = c_3\sigma_2, \tag{2.6}$$

$$\sigma_1\sigma_3 + c_2\gamma_1\gamma_3 = c_1c_3\gamma_2 - s_1s_3, \tag{2.7}$$

$$-s_2\gamma_1 = s_1c_3\gamma_2 + c_1s_3, \tag{2.8}$$

$$-s_2\sigma_3 = -s_3\sigma_2, \tag{2.9}$$

$$s_2\gamma_3 = -s_3c_1\gamma_2 - s_1c_3, \tag{2.10}$$

$$c_2 = -s_1s_3\gamma_2 + c_1c_3 \quad . \tag{2.11}$$

Conditions (2.3)–(2.11) give relations between the values of the rapidity parameters $\{\eta_i\}$ and of the vertex angles $\{\alpha_i\}$. For a generic vertex, only three of the six variables $\{\eta_i\}$ and $\{\alpha_i\}$ represent free parameters. A given set of variables $\{\eta_i\}$ and $\{\alpha_i\}$, which correspond to a solution of the vertex conditions, does not necessarily represent a set of physically meaningful parameters. A solution of the vertex conditions is acceptable when a neighbourhood of the vertex, determined by the values of the parameters $\{\eta_i\}$ and $\{\alpha_i\}$, turns out to be isometrically equivalent to an open domain of Minkowski space. This implies [2] that only one of the three angles $\{\alpha_i\}$ can have a value greater than π. Examples of solutions of the vertex conditions are in order.

Trivial vertex. The vertex conditions admit a simple solution in which all the rapidity parameters are vanishing

$$\eta_1 = \eta_2 = \eta_3 = 0, \tag{2.12}$$

and

$$\alpha_1 + \alpha_2 + \alpha_3 = 2\pi\,. \tag{2.13}$$

The two-dimensional curvature $\mathcal{R}$ associated with a trivial vertex is vanishing

$$\mathcal{R} = 2\pi - \alpha_1 - \alpha_2 - \alpha_3 = 0\,. \tag{2.14}$$

Quasi-static vertex. A non-trivial vertex which is characterized by the variables $\{\eta_i\}$ and $\{\alpha_i\}$ is called quasi-static when one of the rapidity parameters, say η_3, is vanishing. In this case, the vertex conditions admit the solution

$$\eta_1 = \eta, \qquad \eta_2 = \eta, \qquad \eta_3 = 0, \tag{2.15}$$

$$\alpha_1 = \pi - \alpha, \qquad \alpha_2 = \alpha, \qquad \alpha_3 = \pi, \tag{2.16}$$

where η and α (with $0 < \alpha < \pi$) are free parameters. The two-dimensional curvature associated with a quasi-static vertex is given by

$$\mathcal{R} = 0\,. \tag{2.17}$$

Symmetric vertex. When the values of the three rapidity parameters $\{\eta_i\}$ are equal, the vertex is called symmetric. One finds

$$\eta_1 = \eta_2 = \eta_3 = \eta, \tag{2.18}$$

and

$$\alpha_1 = \alpha_2 = \alpha_3 = \alpha, \tag{2.19}$$

with

$$\cos\alpha = -\frac{\mathrm{Ch}\,2\eta}{1 + \mathrm{Ch}\,2\eta}, \qquad \sin\alpha > 0\,. \tag{2.20}$$

Equation (2.20) implies that

$$\frac{2\pi}{3} \leqslant \alpha < \pi\,. \tag{2.21}$$

The two-dimensional curvature $\mathcal{R}$ associated with a symmetric vertex is

$$\mathcal{R} = 2\pi - 3\alpha = -3\left(\alpha - \frac{2\pi}{3}\right), \tag{2.22}$$

and from equation (2.21) it follows that

$$-\pi < \mathcal{R} \leqslant 0\,. \tag{2.23}$$

Quasi-symmetric vertex. A non-trivial vertex is called quasi-symmetric when the absolute values of $\{\eta_i\}$ are equal and one of the three rapidity parameters, say η_3, has opposite sign with respect to η_1 and η_2. In this case, the solution of the vertex conditions is given by

$$\eta_1 = \eta_2 = \eta, \qquad \eta_3 = -\eta, \tag{2.24}$$

and

$$\alpha_1 = \alpha_2 = \alpha, \qquad \alpha_3 = \pi + \alpha \tag{2.25}$$

with

$$\cos\alpha = \frac{\mathrm{Ch}\,2\eta}{1 + \mathrm{Ch}\,2\eta}, \qquad \sin\alpha > 0\,. \tag{2.26}$$

From equation (2.26) one obtains

$$0 < \alpha \leqslant \frac{\pi}{3}\,. \tag{2.27}$$

The two-dimensional curvature associated with a quasi-symmetric vertex is given by

$$\mathcal{R} = \pi - 3\alpha, \tag{2.28}$$

and satisfies the relation

$$0 \leqslant \mathcal{R} < \pi\,. \tag{2.29}$$

3. Tessellation and topology

For each tessellation of the Cauchy surface Σ, one can introduce a topological diagram which describes the structure of the vertices and of the couples of edges which must be identified in the tessellation. For example, the detail of the topological diagram which corresponds to the tessellation of figure 1 is shown in figure 4. Each couple of edges which must be identified in the tessellation is represented by a simple line in the topological diagram; the lines which appear in a topological diagram need not be straight lines and their length is not related to the real length of the edges of the tessellation. Since only 3-valent vertices are present in the tessellation, the associated topological diagram has the structure of a Feynman diagram of a ϕ^3-like field theory. In order to reconstruct the structure of the tessellation associated with a given topological diagram, one can use the double-line representation [15] of the propagators in which the two lines of each propagator represent a couple of edges which must be identified. Consider, for example, the topological diagram of figure 5(a); by introducing the double-line representation of the propagators, one finds the diagram of figure 5(b). Therefore, the corresponding tessellation consists of a single polygon with three couples of edges (which must be identified as shown in figure 5(b)) and two vertices. Consequently, the surface which is described by this tessellation has Euler characteristic χ given by

$$\chi = 2 - 3 + 1 = 0\,. \tag{3.1}$$

In general, consider a topological diagram which has V vertices and P propagators; by using the double-line representation for each propagator, one obtains a diagram in which the set of the all lines is the union of a certain number of connected components that we may call 'loops'. Each of these 'loops' represents a polygon of the corresponding tessellation. Let F be the number of these 'loops'; the surface which is described by the associated tessellation has the Euler characteristic

$$\chi = V - P + F\,. \tag{3.2}$$

Since the Euler characteristic χ of a closed surface Σ_g is related to the genus g of the surface according to

$$\chi = 2 - 2\,g, \tag{3.3}$$

the surface associated with the tessellation described by the topological diagram of figure 5 has genus $g = 1$.

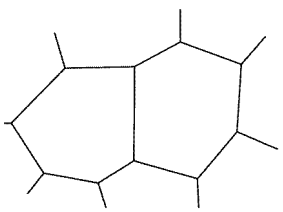

Figure 4. Detail of the topological diagram associated with the tessellation of figure 1.

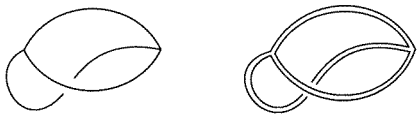

Figure 5. Example of a topological diagram and the corresponding diagram obtained by means of the double-line representation of the propagators.

In order to describe the spacetime geometry of a universe with the topology of $\Sigma_g \times \mathbb{R}$, we only need to produce a specific tessellation of the surface Σ_g at a given time because the time evolution of this surface is determined then by 't Hooft 's rules. The set of data which are associated with a given tessellation contains the lengths $\{ L_i \}$ and the rapidity parameters $\{ \eta_i \}$ of all the edges of the polygons. In the absence of trivial and quasi-static vertices, the variables $\{ L_i , \eta_i \}$ represent a complete set of data. Indeed, when all the rapidity parameters of each vertex are non-vanishing, the vertex angles are uniquely determined by the vertex conditions. For each quasi-static vertex, one needs to add the value of a vertex angle (which is a free parameter). Similarly, for each trivial vertex one has to specify in general the values of two vertex angles.

Let us now consider the constraints on the structure of the topological diagrams which are related to the non-trivial topology of the universe. For any Cauchy surface Σ_g of genus $g \geqslant 1$, one can always construct [2, 8] a tessellation made of a single polygon. The associated topological diagram cannot have an arbitrary number V of vertices and an arbitrary number P of propagators. Indeed, if the topological diagram corresponds to a one-polygon tessellation, the number E of edges of this polygon must be equal to $2P$ and, since there are only 3-valent vertices, it must also be equal to $3V$. Therefore, one obtains

$$E = 2P = 3V \,. \tag{3.4}$$

On the other hand, the value of the Euler characteristic gives the relation

$$\chi = 2 - 2g = V - P + 1 \,. \tag{3.5}$$

Equations (3.4) and (3.5) imply that

$$V = 4g - 2 \,, \tag{3.6}$$

$$P = 6g - 3 \,, \tag{3.7}$$

$$E = 12g - 6 \,. \tag{3.8}$$

Let us now verify that, when conditions (3.6) and (3.7) are satisfied, no further constraint due to the topology of the universe must be imposed.

Let us first recall that the values of the variables $\{ L_i , \eta_i \}$ cannot be chosen arbitrarily because, in 't Hooft's formalism, one has constraints [2, 7]. These constraints state that the polygons of the tessellation must be true polygons. This simply means that the lengths of the edges and the values of the vertex angles must be related in such a way that each polygon is 'closed'. Let us assume, therefore, that conditions (3.6) and (3.7) are satisfied. By imposing the standard constraints related to the closure of the polygons, one gets a tessellation made of a single polygon; in agreement with equation (3.8), this polygon has

$(12g-6)$ edges. Therefore, the sum of all the internal angles $\{\alpha_i\}$ of this polygon is given by

$$\sum_i \alpha_i = \pi\,(E-2) = 4\pi\,(3g-2)\ . \tag{3.9}$$

On the other hand, it is known that the Euler characteristic (3.5) can also be expressed in terms of the two-dimensional curvature which, in our case, may have non-vanishing values only at the vertices of the tessellation. By taking the sum of the two-dimensional curvature associated with the vertices, one finds

$$\begin{aligned}\chi &= \frac{1}{2\pi}\sum_v \mathcal{R}_v = \frac{1}{2\pi}\sum_v \left(2\pi - \alpha_1^{(v)} - \alpha_2^{(v)} - \alpha_3^{(v)}\right) \\ &= V - \frac{1}{2\pi}\sum_i \alpha_i = (4g-2) - 2\,(3g-2) \\ &= 2-2g\,.\end{aligned} \tag{3.10}$$

Equation (3.10) shows that, if the values of the angles are consistent with the closure of the polygon, the sum of the two-dimensional curvatures gives directly the correct value of the Euler characteristic. This means that, in addition to equations (3.6) and (3.7), no further constraint due to the topology of the universe must be imposed.

In the remaining part of this article, we shall consider explicit examples of spacetimes with the topology of $\Sigma_g \times \mathbb{R}$. We shall firstly discuss in detail the case in which $g = 1$; then, we shall give examples of tessellations associated with surfaces of higher genus.

4. Genus one

According to equations (3.6) and (3.7), the topological diagram associated with a one-polygon tessellation of a torus must have two vertices and three propagators; this topological diagram is shown in figure 5. Let us introduce three rapidity parameters $\{\eta_1\,,\ \eta_2\,,\ \eta_3\}$ which correspond to the velocities of the edges. In our conventions, the rapidity parameter is positive when the corresponding edges have a velocity which is directed outside the polygon. The two vertices of the diagram are denoted by V and W as shown in figure 6. For non-vanishing values of the rapidity parameters $\{\eta_1\,,\ \eta_2\,,\ \eta_3\}$, the values of the vertex angles $\{\alpha_1^{(1)}\,,\ \alpha_2^{(1)}\,,\ \alpha_3^{(1)}\}$ of vertex V are uniquely determined by the vertex conditions. The same happens at vertex W; actually, since the two vertices have the same rapidity parameters, the values of the angles $\{\alpha_1^{(2)}\,,\ \alpha_2^{(2)}\,,\ \alpha_3^{(2)}\}$ of W coincide with those of vertex V. The tessellation associated with the topological diagram of figure 6 consists of a single polygon with six edges. This polygon is a real hexagon (i.e. it is 'closed') only when the sum of the internal angles is given by

$$\begin{aligned}\alpha_1^{(1)} + \alpha_2^{(1)} + \alpha_3^{(1)} + \alpha_1^{(2)} + \alpha_2^{(2)} + \alpha_3^{(2)} \ &= \ 2\left(\alpha_1^{(1)} + \alpha_2^{(1)} + \alpha_3^{(1)}\right) \\ &= \ 4\,\pi\,.\end{aligned} \tag{4.1}$$

Equation (4.1) implies that the two-dimensional curvature associated with the vertices V and W must vanish. When all the rapidity parameters of a vertex are non-vanishing, the associated two-dimensional curvature is negative if all the rapidity parameters have the

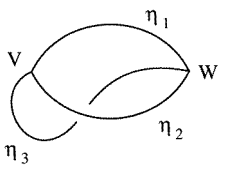

Figure 6. Vertices and rapidity parameters in a topological diagram.

same sign and it is positive in the opposite case. Therefore, in order to have vanishing two-dimensional curvature, the two vertices V and W must be trivial vertices or quasi-static vertices. We shall now analyse these two possibilities separately. Figure 7 shows the structure of the tessellation and its relation with the associated topological diagram.

Static torus. When vertices V and W are trivial vertices, the values of the rapidity parameters $\{\eta_1\,,\ \eta_2\,,\ \eta_3\}$ are vanishing. Therefore, the edges of the polygon are static and the tessellation describes a static universe with the spatial topology of a torus. For each vertex, the sum of the vertex angles must be equal to 2π. There are three couples of edges which must be identified; moreover, one has the constraint that the polygon should be closed. It is easy to verify that any two edges which must be identified must be parallel; this implies that the vertex angles in V and W are equal. To sum up, the hexagon of the tessellation has the form shown in figure 8, where the edges which are labelled by means of the same symbol should be identified. In order to obtain the standard picture of the torus, one can use the construction illustrated in figure 9. Clearly, by varying the lengths of the edges and the values of the vertex angles, one can obtain a static torus with arbitrary values of the Teichmüller parameters.

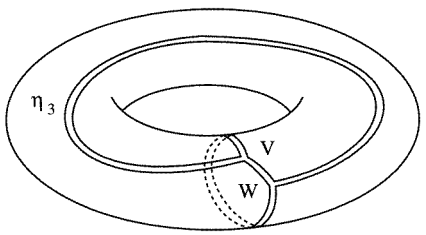

Figure 7. Topological structure of the tessellation of a torus.

Moving torus. Let us now consider the case in which V and W are quasi-static vertices. To simplify the exposition, let us choose η_3 as vanishing rapidity parameter

$$\eta_1 = \eta, \qquad \eta_2 = \eta, \qquad \eta_3 = 0\,. \tag{4.2}$$

With this choice, the two static edges are directed along a longitude of the torus, as shown in figure 7. According to equation (2.16), the values of the vertex angles $\alpha_3^{(1)}$ and $\alpha_3^{(2)}$, which are placed in front of the static edges in the vertices, are equal to π. Closure of the polygon implies that the values of the remaining vertex angles for V and W must coincide

$$\alpha_1^{(1)} = \alpha_1^{(2)} = \pi - \alpha, \tag{4.3}$$

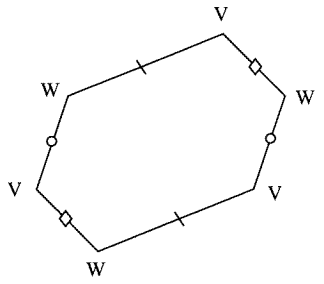

Figure 8. Tessellation of a static torus.

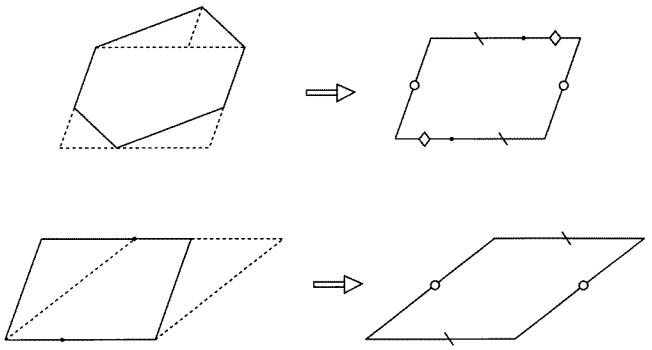

Figure 9. By cutting and gluing along the dashed lines, the hexagon tessellation of figure 8 is transformed into the standard tessellation of the torus with only two couples of edges.

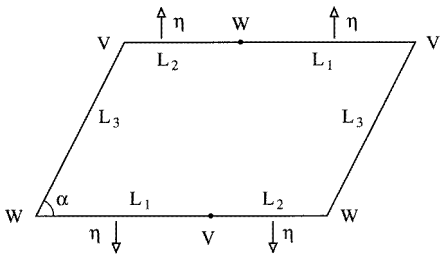

Figure 10. Tessellation of a moving torus.

$$\alpha_2^{(1)} = \alpha_2^{(2)} = \alpha, \tag{4.4}$$

where α is a free parameter with $0 < \alpha < \pi$. We shall consider the case in which $0 < \alpha \leqslant \pi/2$; the extension to the case $\pi/2 < \alpha < \pi$ is straightforward and can also be obtained by means of modular transformations. Consequently, the polygon of the tessellation has the form shown in figure 10. The lengths of the three couples of edges, which must be identified, have been denoted by $\{L_1, L_2, L_3\}$; the two edges with length L_3 are static whereas the edges with lengths L_1 and L_2 are moving and have the same rapidity

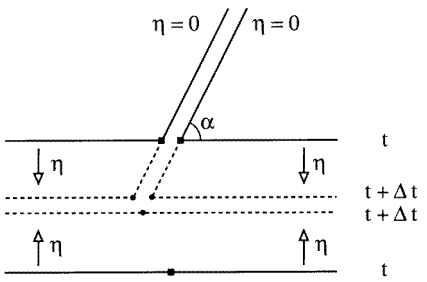

Figure 11. Time evolution of a quasi-static vertex.

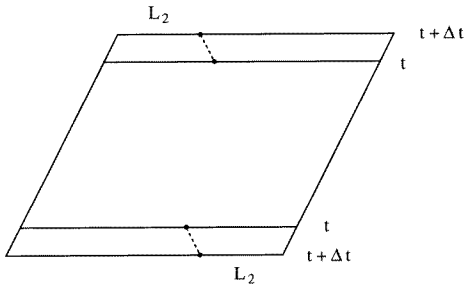

Figure 12. Structure of the tessellation of figure 10 at time t and at time $t + \Delta t$.

parameter η. For positive η the polygon is expanding and the tessellation describes an expanding universe with the spatial topology of a torus.

Suppose that, at some fixed time t, the system is described by the tessellation of figure 10 with $0 < \alpha < \pi/2$. In order to determine the time evolution of the tessellation, we need to consider the motion of the edges and the associated motion of the positions of the vertices. The time evolution of a quasi-static vertex is represented in figure 11 where the positions of the edges at times t and $t + \Delta t$ are shown. Therefore, at time $t + \Delta t$, the structure of the tessellation is given by the polygon shown in figure 12. As time goes by, the length L_2 of two edges which must be identified decreases and, when L_2 vanishes, one has a transition of type A. By using 't Hooft's rules [2] for the transitions, it turns out that the corresponding exchange of vertices V and W is just a slide of these two vertices over the moving edges. The modification of the tessellation in this transition is shown in figure 13, where the size of the polygon at different times $t < t_1 < t_2$ is depicted; the transition occurs precisely at time t_1.

To sum up, the time evolution of the tessellation is described by a uniform expansion of the polygon in the 'y direction'; during this expansion, the positions of the vertices slide over the two horizontal (moving) boundaries and, when they reach the static edges, they jump to the opposite side. So, one has a sequence of infinite transitions with a constant time interval between them. Clearly, when $\alpha = \pi/2$, the lengths L_1 and L_2 are separately constant in time and, consequently, there are no transitions (the positions of the vertices on the moving edges are fixed).

5. Teichmüller parameters

At a fixed time t, the tessellation of the torus is represented in figure 10. We shall consider the case in which the rapidity parameter η is positive, so that the universe is expanding. Let us now introduce the Teichmüller parameters $\{\tau_1, \tau_2\}$ which are related to the size of the polygon as shown in figure 14. According to the standard normalization of the Teichmüller parameters, one gets

$$\tau_1 = \frac{L_2 + L_3 \cos\alpha}{L_1 + L_2}, \tag{5.1}$$

$$\tau_2 = \frac{L_3 \sin\alpha}{L_1 + L_2}. \tag{5.2}$$

In order to determine the time evolution of $\{\tau_1, \tau_2\}$, we need to consider the time evolution of $\{L_1, L_2, L_3\}$ because the value of the angle α is constant in time. The moving edges have velocity w given by

$$w = \mathrm{Th}\,\eta; \tag{5.3}$$

therefore, by using the geometric relations which are consequences of the structure of the polygon and of figure 11, one finds that, within two consecutive transitions, the time derivative of the lengths of the edges takes the form

$$\dot{L}_1 = 2\,\mathrm{Th}\,\eta\ \cot\alpha, \tag{5.4}$$

$$\dot{L}_2 = -2\,\mathrm{Th}\,\eta\ \cot\alpha, \tag{5.5}$$

$$\dot{L}_3 = 2\,\frac{\mathrm{Th}\,\eta}{\sin\alpha}. \tag{5.6}$$

By following the evolution of the tessellation backward in time, one finds the situation in which $L_3 = 0$ and the torus was degenerate. We shall fix the origin of time by requiring that, at $t = 0$, one has $L_3 = 0$ and the universe begins to expand. From equations (5.4)–(5.6) it follows that

$$L_1(t) = L_1(0) + 2\,(\mathrm{Th}\,\eta\ \cot\alpha)\,t, \tag{5.7}$$

$$L_2(t) = L_2(0) - 2\,(\mathrm{Th}\,\eta\ \cot\alpha)\,t, \tag{5.8}$$

$$L_3(t) = 2\left(\frac{\mathrm{Th}\,\eta}{\sin\alpha}\right)t. \tag{5.9}$$

Equations (5.7)–(5.9) describe the uniform expansion of the polygon; in agreement with the structure of the tessellation, the sum $L_1 + L_2$ turns out to be constant in time

$$L_1(t) + L_2(t) = L_1(0) + L_2(0). \tag{5.10}$$

At time t_1 given by

$$t_1 = \frac{L_2(0)\ \tan\alpha}{2\,\mathrm{Th}\,\eta}, \tag{5.11}$$

one has $L_2(t_1) = 0$ and thus a transition takes place. After this first transition and before the second one, one has

$$L_1(t) = L_1(0) + 2\,(\mathrm{Th}\,\eta\ \cot\alpha)\,t - (L_1(0) + L_2(0))\ , \tag{5.12}$$

$$L_2(t) = L_2(0) - 2\,(\mathrm{Th}\,\eta\ \cot\alpha)\,t + (L_1(0) + L_2(0))\ , \tag{5.13}$$

$$L_3(t) = 2\left(\frac{\mathrm{Th}\,\eta}{\sin\alpha}\right)t\ . \tag{5.14}$$

The evolution of the tessellation is described then by an infinite sequence of transitions and, within two consecutive transitions, the lengths of the edges vary linearly in time. The time interval δt between two consecutive transitions is

$$\delta t = \frac{L_1(0) + L_2(0)}{2\,\mathrm{Th}\eta}\ \tan\alpha\ . \tag{5.15}$$

Let us now consider the time evolution of the Teichmüller parameters. By inserting the expressions (5.7)–(5.9) into equations (5.1) and (5.2), for $0 \leqslant t < t_1$ one finds

$$\tau_1(t) = \frac{L_2(0)}{L_1(0) + L_2(0)}\ , \tag{5.16}$$

$$\tau_2(t) = \frac{2\,\mathrm{Th}\,\eta}{L_1(0) + L_2(0)}\ t\ . \tag{5.17}$$

In each transition, the lengths of the edges are modified according to

$$L_1\ \rightarrow\ L_1 - (L_1(0) + L_2(0))\,, \tag{5.18}$$

$$L_2\ \rightarrow\ L_2 + (L_1(0) + L_2(0))\,, \tag{5.19}$$

$$L_3\ \rightarrow\ L_3\,. \tag{5.20}$$

Consequently, in each transition the Teichmüller parameters transform as

$$\tau_1\ \rightarrow\ \tau_1 + 1, \tag{5.21}$$

$$\tau_2\ \rightarrow\ \tau_2\,. \tag{5.22}$$

In the complex upper half-plane of the Teichmüller parameter τ of the torus,

$$\tau = \tau_1 + \mathrm{i}\tau_2, \tag{5.23}$$

the motion of the representative point of the classical state of the universe is shown in figure 15. The increment $\Delta\tau_2$ of τ_2 in the time period (5.15) is given by

$$\Delta\tau_2 = \tan\alpha\,. \tag{5.24}$$

The discontinuities of the curve represented in figure 15 are related to the transitions which enter the time evolution of the tessellation. It should be noted that 't Hooft transitions do not correspond to physical singularities or discontinuities of the spacetime geometry. In 't Hooft's formalism, the presence of transitions in the evolution of the tessellation is simply a consequence of the particular choice of the spacetime foliation, which is defined by means of piecewise flat surfaces. In agreement with this fact, the discontinuities of the curve of figure 15 do not correspond to discontinuities in the moduli space M of the torus. Indeed,

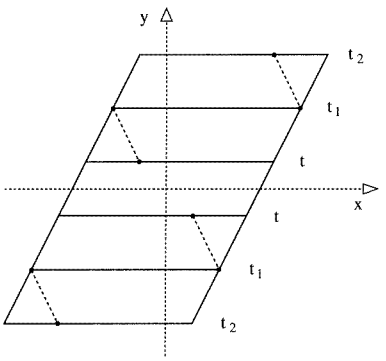

Figure 13. Time evolution of the tessellation of figure 10. A transition of type *A* occurs at time $t = t_1$.

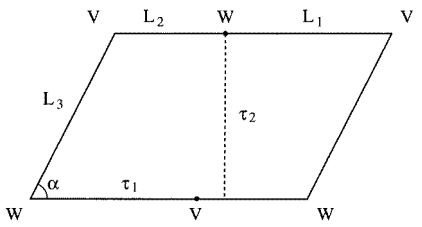

Figure 14. Teichmüller parameters τ_1 and τ_2.

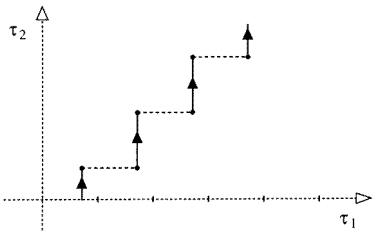

Figure 15. Evolution of the classical state of the universe in Teichmüller space.

the space M can be obtained from the upper half-plane of the Teichmüller parameter τ by factorizing the action of the mapping class group of the torus which can be taken to be generated by the modular transformations

$$\tau \rightarrow \tau + 1\,, \tag{5.25}$$

$$\tau \rightarrow -\frac{1}{\tau}\,. \tag{5.26}$$

In each transition, the modifications (5.21) and (5.22) of the Teichmüller parameters correspond to a modular transformation (5.25); thus, no discontinuities in M are generated by the transitions.

Modulo the action of the transformations (5.25), the curve of figure 15 can be represented by the straight line shown in figure 16 and, under a modular transformation (5.26), this straight line is transformed into the half-circle shown in figure 16. These curves represent geodesic lines with respect to the Poincaré metric of the complex upper half-plane. Thus, one can say that the time evolution of the torus is described by a geodesic in the Teichmüller space equipped with the Poincaré metric. This conclusion is in agreement with the previous results [4–6] obtained by means of the ADM construction.

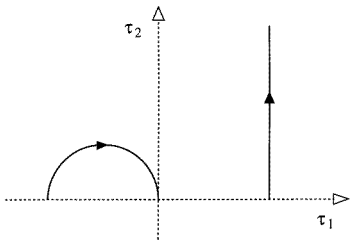

Figure 16. Geodesic curves with respect to the Poincaré metric in Teichmüller space.

In our discussion on the time evolution of the torus, we have chosen η_3 as vanishing rapidity parameter. Clearly, any other choice would not modify the physics of the system. A permutation of the meridian and the longitude of the torus, for example, is equivalent to performing a modular transformation (5.26). With a positive rapidity parameter η, the universe is expanding and the time distance of any event from the initial configuration, in which the torus is degenerate, is finite. Similarly, for negative values of the rapidity parameter η, the universe is contracting and its volume reaches the vanishing value in a finite time. The evolutions of the expanding and of the contracting universes are related by time reversal.

Let us now make a list of the degrees of freedom for the pure gravity system with genus one. The tessellation shown in figure 10 contains five free parameters: the values $\{L_1, L_2, L_3\}$ of the lengths of the edges, the value η of the rapidity parameter and the value α of one of the vertex angles. One variable can be used to fix the overall 'scale' of the distances of the system (the Teichmüller parameters are dimensionless); the remaining four parameters determine the position and the velocity of the representative point in the Teichmüller space. So, the counting of the degrees of freedom in the 't Hooft formalism is in agreement with the counting in the canonical ADM formulation.

6. Covering space

Let us now consider the properties of the tangent space of the universe with the spatial topology of the torus. The effects of a parallel transport of tensors along an oriented path can be described [2, 14] by means of a holonomy matrix $H \in SO(2,1)$ associated with the path; this matrix is defined in the basis specified by the Lorentz frames of the polygons. For a generic path which does not cross the edges of a polygon of the tessellation, the associated holonomy is just the unit matrix. So, we need to specify the holonomy matrix for each possible crossing of the edges. In the case of the static universe described by the tessellation shown in figure 8, the edges have vanishing velocity; consequently, each crossing holonomy

does not boost the vectors and can be given, at most, by a rotation. Since any two edges which must be identified are parallel, each crossing holonomy is actually the unit matrix.

In the case of an expanding universe, the corresponding tessellation is shown in figure 10. The two static edges are parallel; therefore, the holonomy associated with a crossing of these two edges is the unit matrix. Consider now an oriented path $A \to B$ crossing two moving edges, as shown in figure 17. With respect to the coordinate system shown in figure 17, the associated holonomy H is given [2, 14] by a boost in the y-direction with rapidity parameter (-2η)

$$H = \Lambda_2(-2\eta) = \begin{pmatrix} \gamma & 0 & -\sigma \\ 0 & 1 & 0 \\ -\sigma & 0 & \gamma \end{pmatrix}, \tag{6.1}$$

where

$$\gamma = \mathrm{Ch}2\eta, \qquad \sigma = \mathrm{Sh}2\eta\,. \tag{6.2}$$

The physical meaning of the crossing holonomy can be illustrated by means of a simple example. Suppose that a test particle with 3-momentum $\{k^a\}$ hits and crosses the moving edge; after this crossing, the new components $\{k'^a\}$ of its momentum are given by

$$k'^a = [\Lambda_2(-2\eta)]^a{}_b\, k^b\,. \tag{6.3}$$

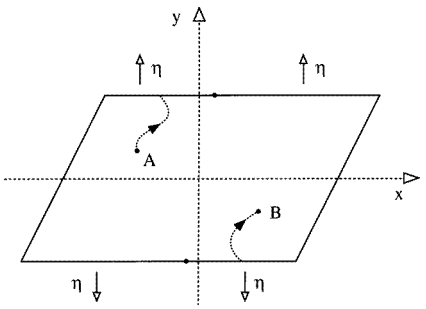

Figure 17. Oriented path $A \to B$ crossing two moving edges.

In order to get a picture of the global structure of the universe, it is useful to produce a presentation of the universe in terms of its universal covering. We shall now describe the covering space associated with the universe with the spatial topology of the torus. Such a presentation, which confirms the internal consistency of 't Hooft's formalism, will be used in the next section. Any simply connected domain with vanishing Riemann tensor is isometrically equivalent to a region of the three-dimensional Minkowski space $\mathcal{M}$. Therefore the universal covering of the spacetime X, which corresponds to a pure gravity system in $(2+1)$ dimensions, can be represented by a region $U \subset \mathcal{M}$. If one denotes by Γ the group of covering translations (automorphisms) acting on U, the spacetime X has a presentation as $X \simeq U/\Gamma$.

When X is the spacetime associated with a static torus Σ_1, X is invariant under time translations. Consequently, we only need to consider the universal covering of the torus

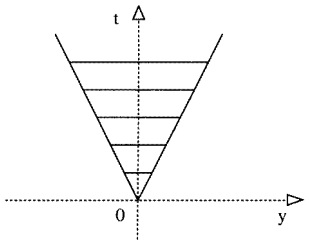

Figure 18. Evolution of the tessellation in the (y, t) plane.

which is given by the plane. So, in this case, U coincides with $\mathcal{M}$ and Γ is generated by the two spatial translations which are associated with the covering of Σ_1.

Let us now consider the more interesting case in which X is the spacetime defined by the expanding torus described in the previous sections. With respect to the reference system shown in figure 17, the moving edges have a velocity $w = \mathrm{Th}\eta$ which is directed along the y-direction. Thus, in the (y, t) plane, the evolution of the tessellation takes the form shown in figure 18. The positions of the moving edges at different times are represented in figure 18 by the two straight lines defined by the equations

$$y = (\mathrm{Th}\,\eta)\ t, \qquad \text{for} \quad t \geqslant 0\,, \tag{6.4}$$

and

$$y = -(\mathrm{Th}\,\eta)\ t, \qquad \text{for} \quad t \geqslant 0\,. \tag{6.5}$$

The x component of the coordinates is not shown in figure 18. Thus, neglecting the x-component of the coordinates, the points of these two straight lines with the same value of the t-coordinate must be identified. It is important to note that these points are related by a Lorentz transformation given by a boost along the y-direction with rapidity parameter (2η). More precisely, consider the point Q_1 on the (y, t) plane with coordinates

$$Q_1 \ \leftrightarrow\ (t_1 = t\ ,\ y_1 = -t\ \mathrm{Th}\,\eta)\ . \tag{6.6}$$

The point Q_1 belongs to a straight line (6.5). Under the transformation described by a boost in the y-direction with rapidity parameter (2η), the coordinates (6.6) are transformed according to

$$(t_1\ ,\ y_1)\ \rightarrow\ (t_2\ ,\ y_2)\ , \tag{6.7}$$

where

$$t_2 = t_1 \mathrm{Ch}2\eta + y_1 \mathrm{Sh}2\eta = t\ , \tag{6.8}$$

$$y_2 = y_1\,\mathrm{Ch}\,2\eta + t_1\,\mathrm{Sh}\,2\eta = t\,\mathrm{Th}\,\eta\,. \tag{6.9}$$

The new variables $(t_2\,,\ y_2)$ can be understood as the coordinates of a new point Q_2 on the (y, t)-plane

$$Q_2 \ \leftrightarrow\ (\,t_2 = t\ ,\ y_2 = t\ \mathrm{Th}\,\eta\,)\ . \tag{6.10}$$

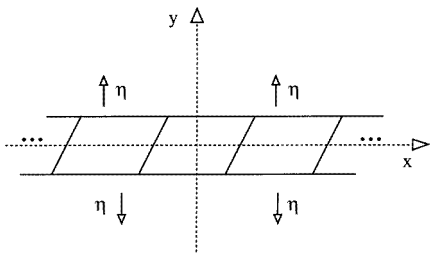

Figure 19. By gluing copies of $\widetilde{X}$ which have been translated in the x-direction, the polygon of figure 17 is transformed into a strip in the (y, x)-plane.

The point Q_2 belongs to the straight line (6.4) and, since it has the same t-coordinate as Q_1, it must be identified with Q_1.

Let us now reconsider the full three-dimensional shape of X. With respect to the Lorentz frame of the polygon, the spacetime X consists of a domain $\widetilde{X}$ of Minkowski space with appropriate identification rules for the points on the boundary of $\widetilde{X}$. We shall construct the universal covering U of X by means of the standard procedure in which U is obtained by gluing suitably transformed copies of $\widetilde{X}$. To take care of the identification of the two static edges, we simply need to add copies of $\widetilde{X}$ which have been translated in the x-direction. After this first step, the polygon of figure 17 is transformed into the strip shown in figure 19. The group of transformations which connect these different copies of $\widetilde{X}$ is generated by a translation $G_1(a)$ in the x-direction

$$G_1(a) = \exp(\mathrm{i}a P_1)\,, \tag{6.11}$$

where

$$P_1 = -\mathrm{i}\frac{\partial}{\partial x}, \tag{6.12}$$

and the translation parameter a is given by

$$a = L_1(t) + L_2(t) = L_1(0) + L_2(0)\,. \tag{6.13}$$

In order to take care of the identification of the moving edges, one cannot simply add copies of $\widetilde{X}$ which have been translated in the y-direction because, as shown in figure 18, these copies would not match. As we have seen before, in order to have matching of the moving edges (neglecting the x-component of the coordinates) one has to use Lorentz transformations generated by a boost in the y-direction with the rapidity parameter (2η)

$$\Lambda_2(2\eta) = \begin{pmatrix} \mathrm{Ch}\,2\eta & 0 & \mathrm{Sh}\,2\eta \\ 0 & 1 & 0 \\ \mathrm{Sh}\,2\eta & 0 & \mathrm{Ch}\,2\eta \end{pmatrix}. \tag{6.14}$$

Thus, by adding an infinite number of copies of $\widetilde{X}$ which have been Lorentz transformed in the y-direction (and, possibly, have also been translated in the x-direction), figure 18 is transformed into figure 20. By taking into account the x-component of the coordinates, the generator G_2 of the group of transformations connecting these copies of $\widetilde{X}$ turns out to be

$$G_2 = \exp(\mathrm{i}bP_1)\,\Lambda_2(2\eta), \tag{6.15}$$

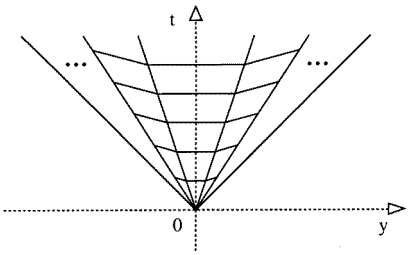

Figure 20. By gluing copies of $\widetilde{X}$ which have been Lorentz transformed in the y-direction, the region of figure 18 is transformed into the cone $|y| \leqslant t$ with $t \geqslant 0$ in the (y, t)-plane.

where the translation parameter b is given by

$$b = L_2(0)\,. \tag{6.16}$$

To sum up, the universal covering $U \subset \mathcal{M}$ of the spacetime X, which corresponds to an expanding universe with the spatial topology of a torus, is given by the set

$$U = \{\,(t\,,\,x\,,\,y\,) \in \mathcal{M}, \quad t \geqslant 0, \quad |\,y\,| \leqslant t\,\}\,. \tag{6.17}$$

The group Γ of covering automorphisms acting on U is the group generated by the isometries G_1 and G_2 given in equations (6.11) and (6.15)

$$\Gamma = \{\,G_1\,,\,G_2\,\}\,. \tag{6.18}$$

The value (6.16) of the translation parameter b is in agreement with the value (5.16) of the Teichmüller parameter τ_1. Moreover, the boost matrix $\Lambda_2(2\eta)$ entering the definition (6.15) of G_2 is the inverse of the crossing holonomy (6.1). This fact is not a coincidence; indeed, as the following argument will show, it represents a consistency condition for the agreement between 't Hooft's formalism and the meaning of the universal covering of the spacetime X.

Since U is a subset of the Minkowski space $\mathcal{M}$, the natural Lorentz frame associated with U is the frame inherited from $\mathcal{M}$. With respect to this coordinate frame, the motion of a test particle in U is free motion because U is flat. Suppose now that one test particle crosses the moving edges of the polygon as shown in figure 21. Region I of figure 21 represents $\widetilde{X}$ and region II represents a copy of $\widetilde{X}$ obtained by means of the Poincaré transformation G_2. With respect to the Lorentz frame of U, the test particle moves on a straight line and has momentum $\{k^a\}$ in both regions. However, when the motion in U is projected into X, one must take into account the relation between the frames of regions I and II. Consequently, with respect to the Lorentz frame of X, the components $\{k'^a\}$ of the particle momentum after the crossing of the moving edges are given by

$$k'^a = \left[\Lambda_2^{-1}(2\eta)\right]^a{}_b\, k^b\,. \tag{6.19}$$

Relation (6.19) is in agreement with equation (6.3) which has been obtained by means of 't Hooft's rules [2, 14].

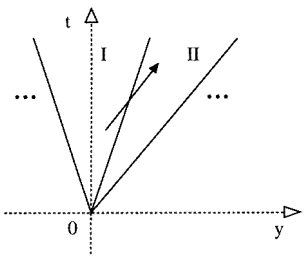

Figure 21. Free motion of a test particle in the universal covering; the particle crosses two moving edges of the tessellation.

7. A topological redshift

The action of the Lorentz transformation (6.19) on the components of the particle momentum, for each crossing of the moving edges of the polygon, gives origin to a peculiar redshift effect. The existence of this general phenomenon in the three-dimensional context was mentioned by Waelbroeck [8] five years ago. In this section, we shall compute the value of the corresponding 'Hubble's constant' in the simple model of an expanding universe with the topology of the torus.

First of all we need to consider how matter can be introduced in 't Hooft's formalism. In the presence of spinless particles, the tessellation contains particles which are placed at the corners of the polygons. Each particle connects two edges of a polygon and these two edges must be identified [2]. We shall consider the case in which the mass m of the particles satisfies the relation $0 \leqslant m < (4G)^{-1}$ where G (with $G > 0$) is the gravitational constant. Each particle introduces a non-trivial two-dimensional curvature given by $\mathcal{R} = 2\beta$ where the deficit angle 2β depends on the energy of the particle. More precisely, if one denotes by E the time component of the 3-momentum of the particle, $p^a = (E\,, \vec{p})$, one has [2]

$$\tan\beta = E\frac{\tan(4\pi Gm)}{m}\,. \tag{7.1}$$

For a massless particle, equation (7.1) becomes

$$\tan\beta = 4\pi GE\,. \tag{7.2}$$

When the values taken by the components of the momentum of each particle are small in gravitational units, i.e. when

$$8\pi G|p^a| \ll 1\,, \tag{7.3}$$

the deficit angles of the particles are small, $\beta \ll 1$. In a topological diagram, the presence of a particle P can be represented as shown in figure 22 and, when equation (7.3) is satisfied, the vertex V of figure 22 can be approximated by means of a quasi-static (or static) vertex. We shall assume that, for each particle, equation (7.3) is satisfied so that the influence of matter on the large-scale structure of the evolution of the universe can be neglected to first approximation. For our illustrative purposes, this approximation is useful because, even in the presence of matter, we can describe the evolution of the universe by means of the

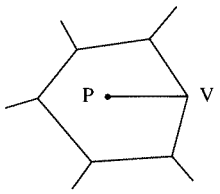

Figure 22. Detail of a topological diagram in the presence of a particle denoted by P.

solution presented in the previous sections and the computation of 'Hubble's constant' turns out to be simple.

Suppose that, at time $t = t_0$, a 'star' emits 'light' with frequency ω_0. We assume that this star is static with respect to the frame of the polygon. This emitted 'light' needs not to be necessarily electromagnetic radiation. To avoid problems with spin, one can imagine that this 'light' is made of spinless particles with zero mass, which propagate with velocity $v = 1$. Suppose that, at time $t = T$ with $T \gg t_0$, this radiation is detected by the apparatus of a static observer; the problem is to find the frequency ω of the detected radiation.

If the time interval $(T - t_0)$ is sufficiently large, the particles of the radiation cross the edges of the expanding polygon several times before reaching the detector. For each crossing of the static edges of the polygon, the energy of these particles is not modified. For each crossing of the moving edges, however, the frequency is modified according to the effects of the boost (6.19) on the components of the momentum. As a result, frequency decreases. Thus, with the topology of a torus, the redshift effect which is produced by the expansion of the universe strongly depends on the direction of the emitted (or absorbed) radiation. In particular, no redshift is observed for the radiation which propagates in the x-direction with respect to the system shown in figure 17. Whereas, the redshift assumes its maximum value for the radiation with velocity directed along the y-direction. We shall therefore concentrate on the latter case.

If the velocity of the massless particles is perpendicular to the moving edges, the frequency ω_2 after one crossing is related to the frequency ω_1 before the crossing according to

$$\omega_2 = \omega_1 \mathrm{e}^{-2\eta} . \tag{7.4}$$

Consequently, after n crossings, the observed frequency ω depends on the emitted frequency ω_0 as

$$\omega = \omega_0 \mathrm{e}^{-2n\eta} . \tag{7.5}$$

We now need to compute the number n of times the radiation crosses the moving edges in its propagation from the source at time $t = t_0$ to the observer at time $t = T$. Since the motion of particles in the covering space is free motion (which is easy to analyse), we shall use the covering space U introduced in the previous section. We only need to consider the (y, t)-plane because the x-component of the coordinates has no influence on n. As shown in figure 23, the source's coordinates are $(t = t_0\,,\ y = 0)$ and the detector's coordinates are $(t = T,\ y = 0)$. The motion in U of the radiated massless particles is described by the straight line connecting the source with point B of coordinates

$$B \ \leftrightarrow\ (t = t_B,\ y = t_B - t_0) . \tag{7.6}$$

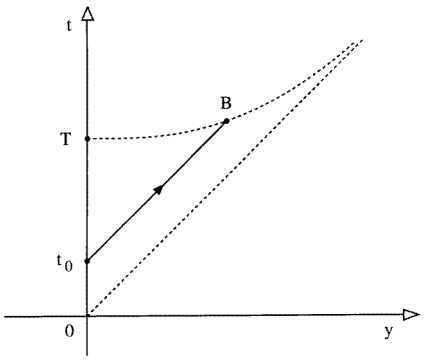

Figure 23. Free motion of radiated massless particles in the covering space. These particles are emitted by the source of coordinates ($t = t_0$, $y = 0$). Point B represents one of the images of the detector in the covering space.

The point B represents the position of one of the images of the detector in the covering space U; therefore, according to the structure (6.15) of the generator G_2 of covering translations, the coordinates of B must be related to the coordinates of the detector by the action of a boost with rapidity parameter $(2n\eta)$

$$t_B = T\ \mathrm{Ch}\,(2n\eta), \tag{7.7}$$

$$t_B - t_0 = T\ \mathrm{Sh}\,(2n\eta)\,. \tag{7.8}$$

Equations (7.7) and (7.8) imply that

$$\begin{aligned} t_0 &= T\big[\mathrm{Ch}\,(2n\eta) - \mathrm{Sh}\,(2n\eta)\big] \\ &= T\,\mathrm{e}^{-2n\eta}\,. \end{aligned} \tag{7.9}$$

Consequently, equation (7.5) reads

$$\omega = \omega_0\,\frac{t_0}{T}\,. \tag{7.10}$$

During its motion from the source to the detector, the radiation is moving with velocity $v = 1$ and, in the reference system of the polygon, it covers a distance L which is given by $L = T - t_0$. Therefore, for the radiation detected in the y-direction, the redshift formula takes the form

$$\frac{\omega - \omega_0}{\omega_0} = \frac{t_0 - T}{T} = -hL\,, \tag{7.11}$$

where the 'Hubble's constant' h is given by

$$h = \frac{1}{T}\,. \tag{7.12}$$

As it was natural to expect, the inverse of the 'Hubble's constant' is precisely the age of the universe.

Because of the angular asymmetry of the topological redshift, the observed spectrum is actually rather complicated. The various images of the source, which are seen by the observer in different directions, present different redshifts and the whole spectrum contains all the corresponding frequencies. Clearly, for a contracting universe, the frequency difference $\Delta\omega = \omega - \omega_0$ is positive and, in this case, one finds a blueshift effect. The frequency shift of the observed radiation is a general phenomenon which is due to the motion of the edges of the polygons of the tessellation; this effect is also present in the case of a universe with the topology of a surface with genus $g > 1$.

8. Higher genus

Let us now consider a spacetime with the topology of $\Sigma_g \times \mathbb{R}$, where Σ_g denotes a Riemann surface of genus $g > 1$. At some fixed time, one can construct a tessellation which consists of a single polygon. During the time evolution, the structure of the tessellation will change and, in general, new polygons may be produced. In order to give examples of spacetimes with topology $\Sigma_g \times \mathbb{R}$ with $g > 1$, we need to find a consistent set of initial data for the tessellation. This problem consists of two parts; firstly, one has to determine the structure of a topological diagram which is consistent with the constraints coming from the non-trivial topology of the universe and, secondly, one must impose the usual constraints which are related to the 'closure' of the polygon. We shall now give a general solution to the first part of this problem.

A topological diagram which describes a one-polygon tessellation of a surface of genus $g \geqslant 1$ must have $(4g-2)$ vertices and $(6g-3)$ propagators. Such a diagram is necessarily non-planar because it must reproduce the correct value of the Euler characteristic of the surface. A topological diagram with the desired properties is shown in figure 24. This diagram consists of a chain of g subdiagrams; each of them is one-particle irreducible. At the beginning and at the end of the chain, there are two OPI subdiagrams with three vertices; whereas each of the intermediate OPI subdiagrams has four vertices. Therefore, the whole topological diagram of figure 24 has the $(4g-2)$ vertices and $(6g-3)$ propagators. Moreover, by using the double-line representation for the propagators, one finds that the tessellation associated with the diagram of figure 24 consists of a single polygon. Consequently, this tessellation describes a surface of Euler characteristic $\chi = 2 - 2g$. Figure 25 shows the structure of the tessellation and its relation with the genus g surface.

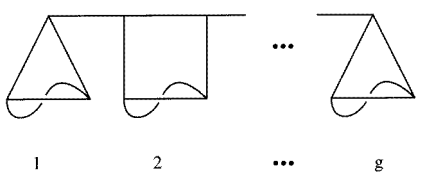

Figure 24. Topological diagram corresponding to a one-polygon tessellation of a surface of genus g.

At this stage, the topological constraints are satisfied and one has to specify the values $\{\eta_i\}$ of the rapidity parameters and the values $\{L_i\}$ of the lengths of all the edges of the polygon. Moreover, one must impose the standard constraints of 't Hooft's formalism that

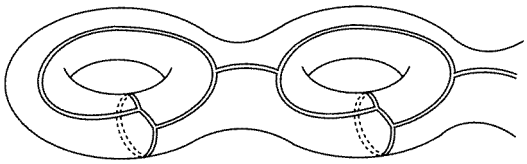

Figure 25. Topological structure of the tessellation of a surface of genus $g \geqslant 2$ which corresponds to the topological diagram of figure 24.

are related to the closure of the polygon. This second part of the problem, which is in general numerically non-trivial, is encountered in the construction of any tessellation. For non-vanishing values of the rapidity parameters, the vertex angles are uniquely determined by the vertex conditions. Since in our case the polygon has $(12g - 6)$ edges, the values $\{\alpha_i\}$ of the angles must satisfy

$$\sum_i \alpha_i = \pi\,(12g - 8)\ . \tag{8.1}$$

Moreover, the lengths of the edges must be chosen in such a way that the polygon is closed. This means that, by using a cyclic ordering to denote the angles and edges of the polygon, the following relation must be satisfied:

$$\sum_j L_j\,\mathrm{e}^{\mathrm{i}\theta_j} = 0\,, \tag{8.2}$$

where

$$\theta_j = \sum_{k=1}^{j-1} (\pi - \alpha_k)\ . \tag{8.3}$$

Once the values $\{\alpha_i\}$ satisfying equation (8.1) have been found, equation (8.2) can be solved in a relatively simple way. Indeed, suppose that the polygon has $2N$ edges; this set of edges consists of N couples of edges that must be identified. One can choose 'freely' the lengths of the first $(N-2)$ couples of edges and the lengths of the remaining two couples of edges are determined by equation (8.2). Thus, the difficulties encountered in the construction of the tessellation are essentially related to the choice of the rapidity parameters because the associated angles should satisfy equation (8.1).

We shall now prove that, for a surface of genus $g \geqslant 2$, a particular solution of 't Hooft's constraints always exists. Since the Riemann surfaces with genus $g \geqslant 2$ have a global (two-dimensional) curvature which is negative, one can choose the values of the rapidity parameters with the same sign. In order to simplify the construction of the solution, one can also require maximal symmetry, i.e. one can impose that all the rapidity parameters take the same value

$$\eta_i = \eta, \qquad \forall\, i = 1\,,\ \ldots\ ,\ (12g - 6)\,. \tag{8.4}$$

In this case, the $(4g-2)$ vertices are equal and symmetric. As we have stated in section 2, in a symmetric vertex the values of the three vertex angles are equal,

$$\alpha_1 = \alpha_2 = \alpha_3 = \alpha, \tag{8.5}$$

where the value of α is given in equation (2.20) and satisfies the relation

$$\frac{2\pi}{3} \leqslant \alpha < \pi . \tag{8.6}$$

In a polygon with $(12g-6)$ edges there are $(12g-6)$ angles. So, in order to satisfy constraint (8.1), the value of α must be given by

$$\alpha = \alpha(g) = \pi \frac{6g-4}{6g-3} . \tag{8.7}$$

As shown in equation (8.7), $\alpha(g)$ is an increasing function of the genus g and the range of values taken by $\alpha(g)$ is given by

$$\pi \frac{8}{9} \quad (\text{for } g=2) \leqslant \alpha(g) < \pi \ (\text{ for } g=\infty) . \tag{8.8}$$

Since the values taken by $\alpha(g)$ satisfy relation (8.6), it is possible to determine the rapidity parameter η by using equation (2.20):

$$\eta = \eta(g) = \tfrac{1}{2} \operatorname{Arch}\left(-\frac{\cos\alpha(g)}{1+\cos\alpha(g)} \right) . \tag{8.9}$$

Thus, when the values of all the rapidity parameters coincide with $\eta(g)$ given in equation (8.9), the values of the angles (which are determined by the vertex conditions) are equal and coincide with $\alpha(g)$ of equation (8.7). In this case, constraint (8.1) is satisfied. Finally, one has to determine the lengths $\{ L_i \}$ of the edges in such a way that condition (8.2) holds. The simplest solution to this last problem consists of taking all the edges with the same length

$$L_i = L, \qquad \forall\, i = 1, \ldots, (12g-6) , \tag{8.10}$$

where L is a free parameter.

To sum up, we have proved that, for a surface of genus $g \geqslant 2$, a particular solution of 't Hooft's constraints always exists. This particular tessellation consists of a regular polygon with $(12g-6)$ edges. The couples of edges which must be identified are determined by the structure of the topological diagram of figure 24. The edges are moving and the associated rapidity parameter is given in equation (8.9). The time evolution of this tessellation corresponds to a conformal expansion or contraction of the regular polygon; therefore, no transitions take place. The existence of this particular solution actually implies the existence of many other solutions which are obtained by means of smooth deformations of the parameters $\{ \eta_i , L_i \}$.

For a generic tessellation of a surface Σ_g of genus $g \geqslant 2$, the time evolution will contain 't Hooft's transitions. Since these local modifications of the structure of the tessellation are not related to singularities or discontinuities in the geometry of spacetime, these transitions must correspond to modular transformations acting on the Teichmüller space of Σ_g. Differently from the case of the torus, a universe with the topology of $\Sigma_g \times \mathbb{R}$ with $g \geqslant 2$ cannot be static with respect to the Lorentz frame of the polygon. Indeed, the two-dimensional curvature of Σ_g is non-vanishing for $g \geqslant 2$; therefore, the geometry of a static universe of the type $\Sigma_g \times \mathbb{R}$ is not consistent with Einstein's equations.

In 't Hooft's formalism, the time evolution of any specific tessellation admits a simple geometric description; indeed, the laws of the dynamics take the form of kinematic relations. Unfortunately, it is rather difficult (in general) to give a detailed analytic description of this evolution because of the presence of constraints (8.1) and (8.2) which ensure the consistency of the initial data. In the case of a universe with the spatial topology of a torus, for example, constraints (8.1) and (8.2) are easy to solve and, consequently, it is possible to give a complete analytic description of the time evolution of the tessellation. For a universe with the topology of $\Sigma_g \times \mathbb{R}$ with $g > 1$, however, the explicit form of the more general solution of constraints (8.1) and (8.2) is difficult to produce. In this case, a numerical analysis based on computer simulations will probably be useful to explore the properties of the system.

We conclude this section with a note on the number of degrees of freedom in a pure gravity system with the topology of $\Sigma_g \times \mathbb{R}$ with $g \geqslant 2$. The surface Σ_g can be described by a tessellation which consists of a single polygon with $(12g-6)$ edges. When the tessellation contains generic vertices with non-vanishing rapidity parameters, the values of the vertex angles are uniquely fixed by the vertex conditions. Therefore, the tessellation is determined by the values of the real variables $\{ \eta_i , L_i \}$. If one ignores constraints (8.1) and (8.2), the set $\{ \eta_i , L_i \}$ actually contains $(12g - 6)$ independent variables because two edges which must be identified have the same length and have the same rapidity parameter.

The parameters $\{ \eta_i , L_i \}$ can be understood [7] as canonical conjugate variables of an Hamiltonian system; the Hamiltonian function is proportional [7] to the two-dimensional curvature and depends on the values $\{ \eta_k \}$ of the 'momenta'. Since relation (8.2) contains non-trivial real and imaginary parts, equation (8.2) introduces two constraints. By taking the time derivative of equation (8.2), one obtains two additional constraints

$$\sum_j \dot{L}_j (\{ \eta_k \}) \, \mathrm{e}^{i \theta_j} = 0 \,, \tag{8.11}$$

where $\{ \theta_j \}$ are given in equation (8.3). Thus, equations (8.2) and (8.11) can be used to eliminate four variables (two 'coordinates' and the two associated 'velocities'). Finally, constraint (8.1) determines the value of the Hamiltonian energy [7] of the system and introduces one relation among the variables. Consequently, the number ν of free parameters is given by $\nu = (12g - 6) - 5 = 12g - 11$. One of these variables can be used to fix the overall scale of the distances of the system. The remaining $(12g - 12)$ variables determine the position and the velocity of the representative point of the classical state of the universe in the Teichmüller space. Therefore, also in the case of a universe with higher genus, the counting of the degrees of freedom in 't Hooft's formalism is in agreement with the counting of the ADM formulation.

The consistency of constraints (8.1) and (8.2) has been proved, on the basis of geometric arguments, by 't Hooft [7]. A simple argument confirms the validity of our counting of the degrees of freedom. In 't Hooft's formalism, constraint (8.2) is compatible with the time evolution of the tessellation [7]; if relation (8.2) is satisfied at the initial time, it is also valid at any time. Since equation (8.2) really represents two constraints, the two associated 'conjugate momenta' must vanish and this is precisely the meaning of equation (8.11).

9. Conclusions

Gravity in (2+1) dimensions represents a simple model in which some of the open problems of general relativity can be studied. In 't Hooft's formalism, the structure of the spacetime

geometry is described by means of a foliation in which the space-like surfaces admit a tessellation made of polygons. This formulation presents interesting features because it is based on the symmetry properties of general relativity in $(2+1)$ dimensions. In this paper we have used 't Hooft's formalism to describe the classical geometry of universes with the topology of $\Sigma_g \times \mathbb{R}$.

We have studied in detail the case of a universe with the spatial topology of a torus and we have shown that 't Hooft's transitions, which appear in the evolution of the tessellation, are related to modular transformations in the Teichmüller space. We have actually presented a complete analytic description of the time evolution of the tessellation. The universal covering of spacetime has been constructed and we have illustrated how this description of spacetime is in agreement with 't Hooft's formalism. We have considered the topological redshift effect which is induced by the non-trivial topology of an expanding universe; the corresponding 'Hubble's constant' has been computed. For universes with the spatial topology of a surface of higher genus, we have given the general structure of the topological diagram which is associated with a corresponding one-polygon tessellation. In the case of a tessellation made of a regular polygon, we have solved the constraints which are related to the consistency of initial data; the resulting evolution corresponds to a conformal expansion or contraction of the universe. Finally, we have discussed the counting of the degrees of freedom in 't Hooft's formalism and we have shown that there is agreement with the counting in the canonical ADM formulation.

Our results confirm the validity of 't Hooft's formalism to describe classical $(2+1)$ gravity. The convenience of this formalism to construct a consistent quantum version of $(2+1)$ gravity remains to be explored.

Acknowledgments

We wish to thank P Menotti, M Mintchev and G Paffuti for useful discussions.

References

[1] Staruszkiewicz A 1963 *Acta Phys. Polon.* **24** 734
Gott J R and Alpert M 1984 *Gen. Rel. Grav.* **16** 243
Giddings S, Abbot J and Kuchar K 1984 *Gen. Rel. Grav.* **16** 751
Deser S, Jackiw R and 't Hooft G 1984 *Ann. Phys.* **152** 220

[2] 't Hooft G 1992 *Class. Quantum Grav.* **9** 1335; 1993 *Class. Quantum Grav.* **10** S79; 1993 *Class. Quantum Grav.* **10** 1023

[3] Arnowitt R, Deser S and Misner C W 1962 *Gravitation; an Introduction to Current Research* ed L Witten (New York: Wiley)

[4] Martinec E 1984 *Phys. Rev.* D **30** 1198

[5] Moncrief V 1989 *J. Math. Phys.* **30** 2907; 1990 *J. Math. Phys.* **31** 2978

[6] Hosoya A and Nakao K 1990 *Class. Quant. Grav.* **7** 163; 1990 *Prog. Theor. Phys.* **84** 739

[7] 't Hooft G 1993 *Class. Quantum Grav.* **10** 1653

[8] Waelbroeck H 1990 *Class. Quantum Grav.* **7** 751; 1990 *Phys. Rev. Lett.* **64** 2222; 1991 *Nucl. Phys.* B **364** 475; 1994 *Phys. Rev.* D **50** 4982
Waelbroeck H and Zertuche F 1994 *Phys. Rev.* D **50** 4966

[9] Achúcarro A and Townsend P K 1986 *Phys. Lett.* **180B** 89
Witten E 1988 *Nucl. Phys.* B **311** 46
Bengtsson I 1989 *Phys. Lett.* **220B** 51
Carlip S 1989 *Nucl. Phys.* B **324** 106; 1990 *Phys. Rev.* D **42** 2647; 1991 *Class. Quantum Grav.* **8** 5
Grignani G and Nardelli G 1991 *Phys. Lett.* **264B** 45; 1992 *Nucl. Phys.* B **370** 491

[10] Carlip S 1992 *Phys. Rev.* D **45** 3584; 1993 *Phys. Rev.* D **47** 4520; 1994 *Class. Quant. Grav.* **11** 31

Anderson A 1993 *Phys. Rev.* D **47** 4458
Carlip S and Nelson J E 1994 *Phys. Lett.* **324B** 299
Louko J and Marolf D 1994 *Class. Quant. Grav.* **11** 311
Kabat D and Ortiz M E 1994 *Phys. Rev.* D **49** R1684
[11] Ashtekar A 1991 *Lectures on Non-Perturbative Canonical Gravity* (Singapore: World Scientific)
Ashtekar A and Romano J 1989 *Phys. Lett.* **229B** 56
Ashtekar A, Husain V, Rovelli C, Samuel J, Smolin L 1989 *Class. Quant. Grav.* **6** L185
[12] Manojlović N and Miković A 1992 *Nucl. Phys.* B **385** 571-86
Marolf D M 1993 *Class. Quant. Grav.* **10** 2625
Ashtekar A and Loll R 1994 *Class. Quant. Grav.* **11** 2417
[13] Nelson J E and Regge T 1989 *Nucl. Phys.* B **328** 190; 1991 *Phys. Lett.* **272B** 213; 1991 *Commun. Math. Phys.* **141** 211; 1993 *Commun. Math. Phys.* **155** 561
Nelson J E, Regge T and Zertuche F 1990 *Nucl. Phys.* B **339** 516
[14] Franzosi R and Guadagnini E 1995 *Nucl. Phys.* B **450** 327
[15] 't Hooft G 1974 *Nucl. Phys.* B **72** 461